doi:10.3788/gzxb20144310.1023002

器件参量对栅极调制碳纳米管冷阴极的影响

雷达[1],孟根其其格[1],红鸽[1],陈雷锋[2],梁静秋[3],王维彪[3]

(1 内蒙古大学 鄂尔多斯学院,内蒙古 鄂尔多斯 017000)

(2 杭州电子科技大学 材料与工程学院,杭州 310018)

(3 中国科学院长春光学精密机械与物理研究所,长春 130033)

摘 要:基于电场叠加原理,利用悬浮球模型给出了带栅极纳米管顶端电场与电场增强因子,分析了碳纳米管与衬底之间的接触电阻、器件几何参量以及阴栅极之间的电介质对器件场发射性能的影响. 结果表明:接触电阻大大降低了碳纳米管阴极的场发射电流,当接触电阻超过 100 kΩ 时,发射电流密度非常小,此时需要更高的阳极开启电压;当阴栅极之间的电介质为真空时,阴极电子发射性能最佳;除了碳纳米管的长径比之外,栅孔半径、阴栅极间距以及阳极距离等的优化设计,也能提高器件发射性能;通过栅极偏压的调制,可以降低阳极驱动电压.

关键词:碳纳米管;冷阴极;悬浮球;场发射;接触电阻;电介质

中图分类号:O46 **文献标识码**:A **文章编号**:1004-4213(2014)10-1023002-8

The Effects of Parameters for the Field Emission from Gated Carbon Nanotube Cold Cathode

LEI Da[1], MENGGEN Qi-qi-ge[1], HONG Ge[1], CHEN Lei-feng[2], LIANG Jing-qiu[3], WANG Wei-biao[3]

(1 *Ordos College of Inner Mongolia University, Inner Mongolia University, Ordos, Inner Mongolia* 017000, *China*)

(2 *College of Materials and Environmental Engineering, Hangzhou Dianzi University, Hangzhou* 310018, *China*)

(3 *Changchun Institute of Optics, Fine Mechanics and Physics, Chinese Academy of Sciences, Changchun* 130033, *China*)

Abstract: The model of floated sphere in the triode configuration was proposed and the actual electric field and the field enhancement factor at the top of carbon nanotube were calculated analytically by superposition principle of electric field. The effects of the contact resistance, the geometrical parameters of device, and the dielectric of between the gate and cathode were computed. The calculation results show that the emission current from carbon nanotube is greatly reduced by the contact resistance. When the contact resistance is larger than 100 kΩ, the emission current from carbon nanotube tends to be zero. The field enhancement factor was at a maximum value under the condition of the vacuum. The gate-hole radius, the gate-cathode distance, and the gate-anode distance greatly affect the field emission properties of the device. The field emission properties improved via optimizing the parameters above mentioned and modulating the gate voltage.

Key words: Carbon nanotube; Cold cathode; Floated sphere; Field emission; Contact resistance; Dielectric

OCIS Codes: 230.0250; 160.4236; 220.4241; 310.6805; 120.2040

Foundation item: The National Natural Science Foundation of China (No. 61261004)

First author: LEI Da (1973—), male, professor, Ph. D. degree, mainly focuses on nanomaterials and nanotechnology. Email:leida126@126.com

Received: Jan. 17, 2014; **Accepted**: Apr. 10, 2014

0 Introduction

The carbon nanotubes have been considered as one kind of the best electron-emitting materials for vacuum microelectronic devices due to their remarkable field emission properties[1-2]. Their excellent structure, unique mechanical and electrical properties lead to the enhancement of the electric field on the top of the nanotubes. The emission electrons can penetrate through the potential barrier into the vacuum through the tunneling effect[3-4], and a high current density appears at low electric field. Arrays of vertically aligned Carbon Nanotubes (CNTs) have been grown within patterned areas[5-6]. These field emission cold cathodes are suitable for optoelectronic applications such as flat-panel displays, field emission electron sources, and microwave power amplifiers, etc.[7]

Recently, the preparation of gated structures and triodes by using nanopillars or CNT's act as emitters for devices were reported[8-10]. A number of field emitters with a closed hemispherical or hemi-elliptic top have been modeled[11-13] to obtain the potential distribution. Studies have shown that the aspect ratio of emitters could be influence the field emission properties of the nanotubes[14-16]. In our previous works[17-18], the field emission properties on the conductive nanoemiter were studied based on Laplace equation. Although the calculation methods above mentioned are successful in calculating the field distribution, there is a need for model systems, which can be solved analytically, and from which the variations of the actual electric field, the enhancement factor, and the emission current for various parameters can be easily determined. The shape of the emission tip was the hemisphere or hemiellipsoid in the practical devices[11-13] and the experimental results[20] show that the contact resistance between CNT and cathode strongly affects the field emission from CNT.

In this paper, to understand practically the field-emission properties of the gated carbon nanotube cold cathode devices, a model of gated CNT having a cylindrical shape and the hemispherical top was proposed. The actual electric field and the field enhancement factor at the top of CNT were calculated analytically by superposition principle of electric field in the floated sphere model under the condition of the contact resistance and the dielectric between the gate electrode and the cathode were considered. The actual electric field at the top of CNT is expressed easily. Then, the effects of the contact resistance, the geometrical parameters of device, the dielectric between the gate electrode and the cathode on the actual electric field and the field enhancement factor at the top of CNT, field emission current from CNT are investigated.

1 Modeling and calculations

1.1 Model

To research the field emission properties for the gated carbon nanotube on the cathode, we used the model system of triode configuration shown in Fig. 1, in which the carbon nanotube stands perpendicularly on the infinite cathode plane and is placed under the center of the circular gate-hole with the radius of R, having a cylindrical shape of the height h and hemispherical top with the radius of r_0. The space between the gate-electrode and cathode is d_g, the anode-cathode distance is d_a, and which satisfy the conditions of h, $R \gg r_0$, $d_g > h$ and $d_a \gg h$.

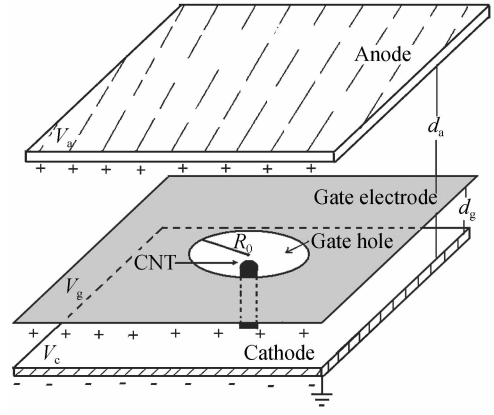

Fig. 1 The model system of a normal-gated CNT cold cathode device

In order to simulate the field emission from gated carbon nanotube, we assume that the sizes of all the plates including anode plate, cathode plate and gate-electrode are much larger than r_0, h, R, d_g, and d_a, and neglecting the space charge effect emission from CNT and the edge effects of all plates during the calculation. The anode voltage is V_a, the gate voltage is V_g, and the cathode voltage is V_c which is maintained at zero ($V_c = 0$). In this case, the influence of gate electrode thickness is neglected and CNT is conductor, and the contact resistance between the cathode and CNT is R_0.

1.2 Potential distribution near the top of CNT

Owing to the macroscopic electric field, almost all the induced charges are exiting at and near the top of carbon nanotube. Thus, the hemisphere and the cylinder under the hemisphere with the length of r_0 can be replaced by the sphere with the radius of r_0 and charge of $-Q$. As the field emission from the CNT is concentrated at the tip, a simpler grounded sphere model of the emitter is proposed as shown in Fig. 2, in which the lower cylinder is replaced by a thin straight wire connected to the bottom of the sphere and

cathode, and R_0 denotes the contact resistance of between the cathode and CNT. When the aspect ratio of carbon nanotube is large enough, this should be a reasonable approximation to the case of Fig. 1.

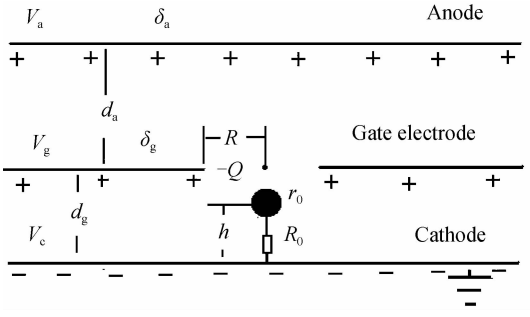

Fig. 2 The grounded sphere model of the normal-gated CNT cold cathode device

In the triode configuration, we can see the potential distribution near the top of CNT is decided by the sum of two parts of potential including the potential near the top of CNT in the diode structure shown in Fig. 3 (which is the model in Fig. 2 when without gate electrode) and the contribution of the gate-electrode to the potential at the point near the top of CNT based on superposition principle of electric field. Hence, in the following paragraphs, to calculate the potential distribution near the top of CNT in triode configuration, the potential distribution near the top of single CNT is calculated by the floating spheres model combining with the image method under the condition of the anode-cathode distance being infinite compared to height of CNT in the diode structure, and the contribution of the gate electrode to the potential at the point near the top of CNT can also be solved analytically. In the above model, the thin wire can be taken away after the sphere reached the cathode. Because the grounded wire hardly influences the distribution of the potential and the field at the apex of the sphere, the calculation for field emission is concentrated at the tip of carbon nanotube, the floated sphere model is thought to be suitable to solve the field emission from carbon nanotube.

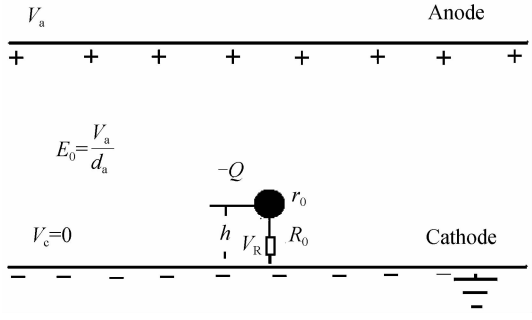

Fig. 3 The two dimensional model of the single CNT on the cathode plane

In order to solve the potential near the top of CNT in the diode structure, we use an even simpler model shown in Fig. 4 and the image method shown in Fig. 5, in which Fig. 4 shows the floated sphere model of individual CNT in the diode structure, and Fig. 5 shows the calculation model of the individual CNT with image method.

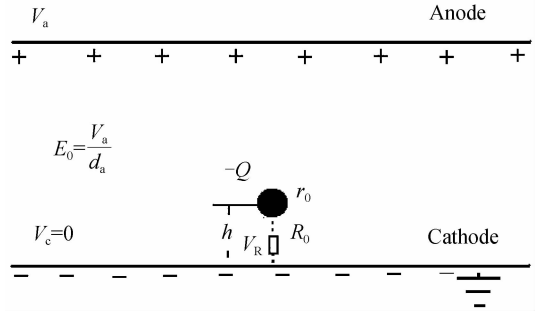

Fig. 4 The floated sphere model of individual CNT in the diode structure

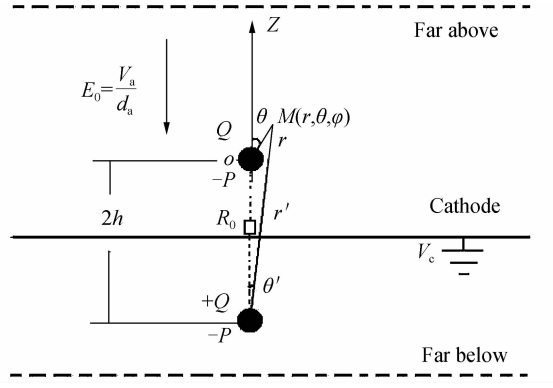

Fig. 5 The calculation model of CNT with image method in diode structure

When the anode-cathode distance is much larger than the height of CNT, we follow Miller[20] in using the image charge shown in Fig. 5. Based on the uniqueness theorem, the field produced by the image must satisfy the boundary conditions at the conductor surfaces. A charge $-Q$ and a dipole $-P$ in the vertical direction were presumed at the center of the sphere. In order to keep the potential of the cathode at the same value with the ground, the image charge $+Q$ and the image dipole $-P$ were introduced at the symmetrical point. Taking the sphere center as the origin O, and the vertical axis through O as the Z axis, $M(r,\theta,\varphi)$ denotes the spherical coordinates of any point in space. Then the potential at $M(r,\theta,\varphi)$ near the top of the sphere should be expressed as

$$\Phi_0(r,\theta,Q)=\frac{1}{4\pi\varepsilon_0}\left\{-\frac{Q}{r}-\frac{p\cos\theta}{r^2}+\frac{Q}{r'}-\frac{p\cos\theta'}{r'^2}\right\}+E_0(h+r\cos\theta) \quad (1)$$

where (r',θ',φ') denote the coordinates of the same point M when another origin at the opposite point of the sphere center, $r'^2=(2h)^2+r^2+2(2hr)\cos\theta$, $r'\cdot\cos\theta'=2h+r\cos\theta$ and $E_0=V_a/d_a$. If r is the same order of magnitude as r_0, up to the first order of r/h we have 1/

$r'=\left(1-\frac{r}{2h}\cos\theta\right)/2h$, $r'\cos\theta'=2h\left(1+\frac{r}{2h}\cos\theta\right)$.

Combining to Eq. (1), the potential around the top of the sphere in diode structure can be expressed as

$$\Phi_0(r,\theta,Q)=\frac{-Q(1-r/2h)}{4\pi\varepsilon_0 r}+E_0 h+E_0 r\cos\theta-p\cos\theta/4\pi\varepsilon_0 r^2 \quad (2)$$

In the following section, we assume that the gate-electrode A with a uniformity charge density of $+\delta_g$ is composed of an infinite electrode B with the uniformity charge density of $+\delta_g$, a circular plate C with the uniformity charge density of $-\delta_g$ and radius of R as shown in Fig. 6, in which the charge density could be obtained by $\delta_g=\varepsilon_0[\varepsilon_r V_g/d_g-(V_a-V_g)/(d_a-d_g)]$ based on electrostatic method on the model in Fig. 2, where ε_0 is the dielectric constant of vacuum and ε_r is the relative dielectric constant of dielectrics. The equivalent structure of the gate-electrode A should be expressed as $(B+C)$ in Fig. 6. Thus, the contribution of the gate-electrode A to the potential at the point $M(r,\theta,\varphi)$ near the top of the sphere is equal to the sum of the potential of infinite electrode B and circular plates C at the same point $M(r,\theta,\varphi)$. The potential of the isolated infinite electrode B with potential of V_g and charge density of $+\delta_g$ at the point M which spaced from the infinite electrode as $(d_g-h-r\cos\theta)$ is obtained by $V_g-(d_g-h-r\cos\theta)\delta_g/2\varepsilon_0$.

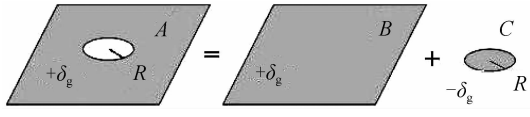

Fig. 6 The schematic of equivalent structure of the gate-electrode

The calculation model for the potential of circular plate C with the uniformity charge density of $-\delta_g$ and radius of R at the point P on the Z axis is shown in Fig. 7, and the potential of the circular plate C with the uniformity charge density of $-\delta_g$ and the radius of R at the point $P(r\cos\theta, 0, 0)$ on Z axis could be obtained based on the electrostatic method,

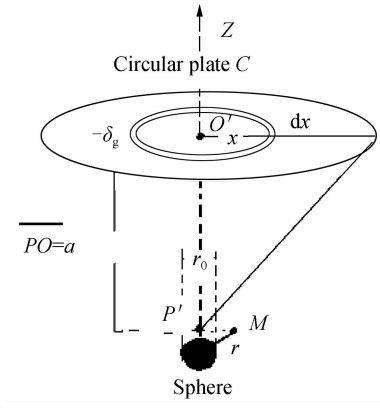

Fig. 7 Calculation model for the potential of circular plate C at the point P on Z axis

$$V_p=\int dV=\int_0^R\frac{-\delta_g\cdot 2\pi x\cdot dx}{4\pi\varepsilon_0\sqrt{x^2+a^2}}=-\frac{\delta_g}{2\varepsilon_0}\cdot(\sqrt{R^2+a^2}-a) \quad (3)$$

where a is the space between the point P and the center of circular plate, and $a=d_g-h-r\cos\theta$. Accurate to the first order terms of r in Taylor series expansion of $\sqrt{R^2+(d_g-h-r\cos\theta)^2}$ as r is very small compared to h, so Eq. (3) could be expressed as

$$V_p=-\frac{\delta_g}{2\varepsilon_0}\cdot\left\{\sqrt{R^2+(d_g-h)^2}-d_g+h+\left[1-\frac{(d_g-h)}{\sqrt{R^2+(d_g-h)^2}}\right]r\cos\theta\right\} \quad (4)$$

In this work, the contribution of the circular plate with uniformity charge density of $-\delta_g$ and the radius of R to the potential at the point $M(r,\theta,\varphi)$ near the top of sphere could be expressed by Eq. (4) approximately, because $R\gg r_0$ and r can be close to the sphere radius r_0 (namely, the point near the top of sphere is close to the point on Z axis). Thus, according to the above mentioned two parts of potential, the contribution of the gate-electrode A to the potential at the point $M(r,\theta,\varphi)$ near the top of the sphere could be obtained,

$$V_M=V_g-\frac{\delta_g}{2\varepsilon_0}\left[\sqrt{R^2+(d_g-h)^2}-\frac{(d_g-h)}{\sqrt{R^2+(d_g-h)^2}}r\cos\theta\right] \quad (5)$$

Hence, combining to Eqs. (2) and (5), the potential distribution at the point $M(r,\theta,\varphi)$ near the top of CNT in the triode is finally obtained as

$$\Phi_0(r,\theta,Q)=[E_0-\frac{p}{4\pi\varepsilon_0 r^3}+[\varepsilon_r(d_a-d_g)(d_g-h)\cdot V_g-(V_a-V_g)(d_g-h)d_g]/[2d_g(d_a-d_g)\cdot\sqrt{R^2+(d_g-h)^2}]]r\cos\theta-\frac{Q(1-r/2h)}{4\pi\varepsilon_0 r}+E_0 h+V_g-\frac{\varepsilon_r V_g}{2d_g}\sqrt{R^2+(d_g-h)^2}+\frac{(V_a-V_g)}{2(d_a-d_g)}\sqrt{R^2+(d_g-h)^2} \quad (6)$$

Due to the existence of the contact resistance between the cathode and carbon nanotube, the potential at the sphere surface is larger than the potential of cathode. The potential at the sphere surface can be obtained from Ohm′s law $V_R=IR_0>0$, where I denotes the electric current from CNT during the field emission process of cold cathode device. The boundary condition of $\Phi_M(r,\theta,Q)=V_R$ at the sphere surface $(r=r_0)$ gives

$$Q\cong 4\pi\varepsilon_0 r_0[E_0 h+V_g-\frac{\varepsilon_r V_g}{2d_g}\sqrt{R^2+(d_g-h)^2}+\frac{(V_a-V_g)}{2(d_a-d_g)}\sqrt{R^2+(d_g-h)^2}]$$

$$p=4\pi\varepsilon_0 r_0^3\left\{E_0+\left[\frac{\varepsilon_r V_g}{d_g}-\frac{(V_a-V_g)}{(d_a-d_g)}\right]\cdot\right.$$

$$\frac{(d_g-h)}{2\sqrt{R^2+(d_g-h)^2}}\Bigg\} \tag{7}$$

we assumed that the equation $(1-r_0/2h)\approx 1$ because CNT has a higher aspect ratio.

1.3 Actual electric field at the top of gated CNT

The electric field at the surface of the floated sphere is calculated from the electric potential grads formula of $E=-\nabla\Phi$ combining to Eq. (6)

$$E=E_r=-\frac{\partial\Phi_M}{\partial r}\bigg|_{r=r_0}=-(A\cos\theta+B\rho-\frac{I}{r_0}\cdot R_0) \tag{8}$$

where

$$\begin{cases} A=3E_0+\dfrac{3(d_g-h)}{2\sqrt{R^2+(d_g-h)^2}}\left[\dfrac{\varepsilon_r V_g}{d_g}+\dfrac{(V_a-V_g)}{(d_a-d_g)}\right] \\ B=\left[E_0+V_g/h-\dfrac{\varepsilon_r V_g}{2d_g h}\sqrt{R^2+(d_g-h)^2}+\dfrac{(V_a-V_g)}{2h(d_a-d_g)}\sqrt{R^2+(d_g-h)^2}\right] \\ \rho=h/r_0 \end{cases} \tag{9}$$

ρ is the aspect ratio of the CNT. Thus, the electric field intensity at the top of the floated sphere (the apex of CNT) could be obtained from Eq. (8) at $\theta=0$, as

$$E_a=|E|_{\theta=0}=\lambda\cdot V_a+\eta\cdot V_g-\frac{I}{r_0}\cdot R_0 \tag{10}$$

where, λ and η are the functions of the geometrical parameters of the device and denote the anode field correlation factor and gate field correlation factor respectively[10], which are determined by

$$\begin{cases} \lambda=\dfrac{1}{d_a}\left[3+\rho+\dfrac{3d_g(d_g-h)}{2(d_a-d_g)\sqrt{R^2+(d_g-h)^2}}+\dfrac{d_g\sqrt{R^2+(d_g-h)^2}}{2r_0(d_a-d_g)}\right] \\ \eta=\dfrac{1}{r_0}+\dfrac{3(d_g-h)}{2\sqrt{R^2+(d_g-h)^2}}\left[\dfrac{\varepsilon_r}{d_g}-\dfrac{1}{(d_a-d_g)}\right]-\dfrac{1}{2r_0}\left[\dfrac{\varepsilon_r}{d_g}+\dfrac{1}{(d_a-d_g)}\right]\sqrt{R^2+(d_g-h)^2} \end{cases} \tag{11}$$

2 Calculating for field enhancement factor

The field enhancement factor β is defined by $\beta=E_a/E_m$[11], where E_a is the actual electric field at the apex of the carbon nanotube and Em is the macroscopic applied electric field. Using this model, we can see the extra electric field is $E_0=V_a/d_a$, which is considered as the corresponding macroscopic applied electric field of the gated structure in this study. Thus the field enhancement factor is given by

$$\beta=3+\rho+W \tag{12}$$

where $\beta_0=3+\rho$ expresses the field enhancement factor of the individual carbon nanotube on the diode structure[20], and W denotes the contribution of gate-electrode for the field enhancement factor on the triode and is a function of the geometrical parameters of the device, the anode and gate voltages

$$W=\frac{d_a V_g}{r_0 V_a}+\left[\frac{1}{(d_a-d_g)}-\frac{V_g}{V_a(d_a-d_g)}+\frac{\varepsilon_r V_g}{d_g V_a}\right]\frac{3(d_g-h)d_a}{2\sqrt{R^2+(d_g-h)^2}}+\left[\frac{1}{(d_a-d_g)}-\frac{V_g}{V_a(d_a-d_g)}-\frac{\varepsilon_r V_g}{d_g V_a}\right]\frac{d_a\sqrt{R^2+(d_g-h)^2}}{2r_0} \tag{13}$$

3 Results and discussions

In Eq. (9), we can see the field correlation factors λ and η are one of the constants because the geometrical parameters of device are invariable during the emission process on the field emission cold cathode device. Thus, the actual electric field and emission current on the top of CNT are mainly determined by the contact resistance, the anode and gate voltages in this case.

The equipotential distribution near the top of CNT in the triode configuration is given in Fig. 8. The actual electric field strength is the maximum at the top of CNT, so we consider the field emission current produced from the top of CNT mainly.

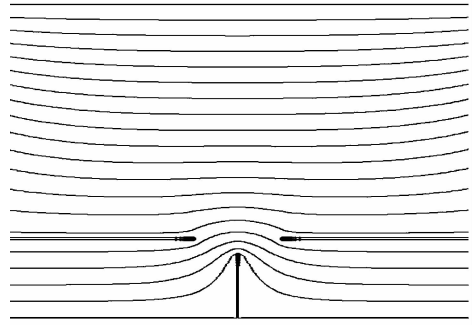

Fig. 8 Equipotential distribution near the top of gated CNT

The field enhancement factor as the functions of the geometrical parameters are calculated and their variation behaviors are discussed as the gate and anode voltages are 300 V and 3 000 V. The variation curves of the field enhancement factor versus gate-anode distance $d_{ag}=d_a-d_g$ are calculated at $d_a=2\ 000\ \mu m$, $r_0=0.02\ \mu m$ and different gate-hole radius 1 μm, 3 μm and 5 μm, respectively, which is given in Fig. 9. The solution result shows that the field enhancement factor increases with the decreasing of the gate-hole radius and the gate-anode distance remarkably.

The variation behavior of field enhancement factor versus the gate-cathode distance dg at different dielectrics (different relative dielectric constant $\varepsilon_r=1$, 1.5, 2) is computed as shown in Fig. 10. The field enhancement factor decreases with the increasing of the gate-cathode distance and is a maximum value under the condition of the vacuum (at $\varepsilon_r=1$).

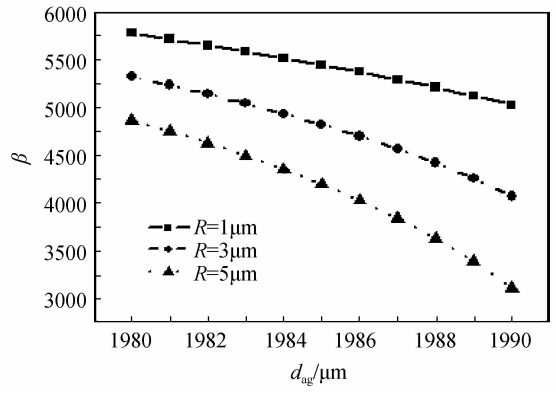

Fig. 9 Variation behavior of field enhancement factor versus the gate-anode distance dag at different gate-hole radiuses

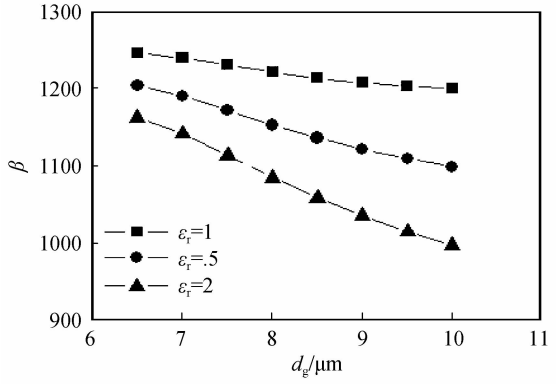

Fig. 10 Variation curves of the field enhancement factor versus gate-cathode distance dg at different dielectrics

In our model, the field enhancement factor becomes $\beta_0 = 3 + \rho$ when without gate-electrode, namely, as $W=0$. Fig. 11 shows the variation curves of the field enhancement factor versus the top radius of carbon nanotube on the triode ($W\neq 0$) and diode ($W=0$) structures. The field enhancement factor increases rapidly as the top radius of carbon nanotue decreases. The field enhancement factor on the triode is much larger than the diode structures, which explains the field emission properties improves via the gate-electrode.

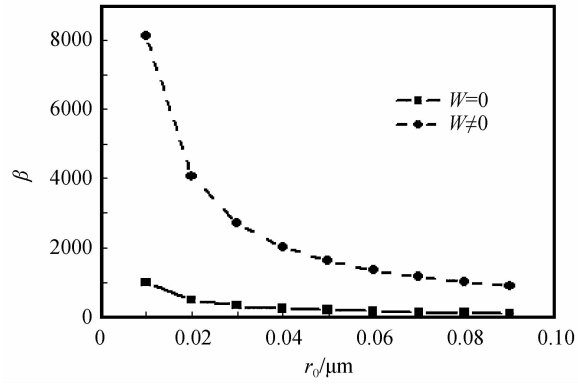

Fig. 11 Variation curves of the field enhancement factor versus the top radius of carbon nanotube on the triode and diode structures

On the other hand, the field emission current I could be obtained from the formula of Fowler-Nordheim

$$I = I_{FN} = 1.54\times 10^{-6}\frac{E^2}{\phi}S \cdot \exp\left(-\frac{6.83\times 10^7 \cdot \phi^{3/2}}{E}\right) \quad (14)$$

where E is the actual electric field at the effective emission surface of the emitter, ϕ is the work function of the effective emission surface and S is the effective emission area of the emitter.

To investigate the effect of contact resistance R_0 for the actual electric field and emission current on the top of CNT, we assumed that the effective emission area is about πr_0^2, $E=E_a$, and the work function of the top surface of CNT is about 5 eV. Then, combining to Eq. (9) it can be obtained

$$E_a = \lambda V_a + \eta V_g - 0.308\times 10^{-6} R_0 S\frac{E_a^2}{r_0} \cdot \exp\left(-\frac{7.636\times 10^6}{E_a}\right) \quad (15)$$

Eq. (15) gives the relation of the contact resistance and actual electric field, according to this equation, the actual electric field at the top of CNT as a function of the contact resistance was calculated at $d_g = 10$ μm, $d_a = 1\,000$ μm, $h = 9$ μm, $r_0 = 0.02$ μm, $R = 5$ μm, $V_a = 3\,000$ V, and different gate voltages $V_g = 200$, 250 and 300 V, as shown in Fig. 12. The actual electric field at the apex of CNT decreased rapidly with the increasing of contact resistance between CNT and cathode. The actual electric fields attained 1.07×10^8, 1.32×10^8 and 1.5×10^8 V/cm for the different gate voltages 200, 250 and 300 V when the contact resistance is zero, which denoted that the field emission properties should be improved through the modulating of gate voltage. Furthermore, the actual electric fields are less than 107 V/cm (it is the threshold electric field) as the contact resistances are larger than 869, 1 093.9 and 1 318.4 kΩ versus gate voltages in above, namely , which explains the electron emission can not

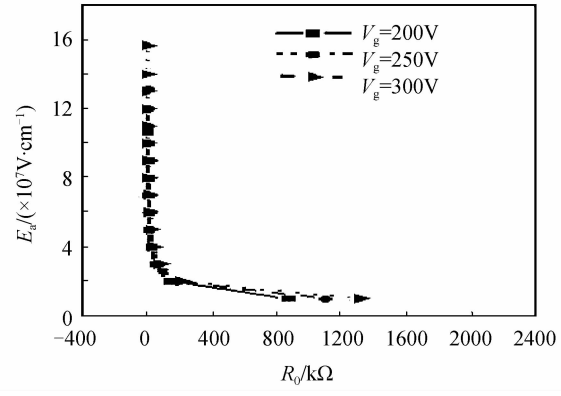

Fig. 12 The variation behavior of actual electric field at the apex of CNT versus the contact resistance R_0

accrues from the emission surfaces in this time.

The relationship between the contact resistance and emission current from CNT is also obtained based on Eqs. (10) and (15), as

$$I=0.308\times10^{-6}S\cdot\left(E_{a0}-\frac{R_0}{r_0}I\right)^2\cdot \exp\left(-\frac{7.636\times10^6}{E_{a0}-IR_0/r_0}\right) \quad (16)$$

where, $E_{a0}=\lambda\cdot V_a+\eta\cdot V_g$ is the actual electric field without contact resistance.

Based on Eq. (16), the field emission current as a function of contact resistance between CNT and cathode was calculated at the different gate voltages of V_g = 150, 250 and 300 V respectively, and their variation behaviors are given in Fig. 13. The contact resistance strongly affects the emission current from CNT. The emission current decreases quickly with the increasing of the contact resistance and tends to be zero when the contact resistance is larger than 100 kΩ. Thus, we know depressing the contact resistance is an important work for the design and preparation process of CNT cold cathode devices. The emission current increases with the gate voltage remarkably at the region of the smaller contact resistance, which expresses the threshold voltage of anode could be reduced by via concocting the gate voltage, but the emission current does not increase evidently in the region of the larger contact resistance.

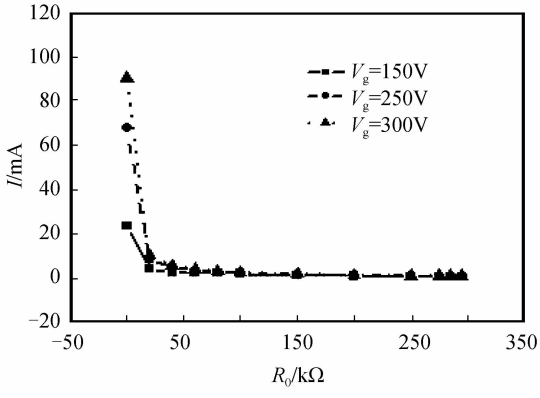

Fig. 13 The curves of field emission current I as a function of contact resistance R_0 at different gate voltages

Fig. 14 shows that the field emission current from CNT as a function of gate voltage V_g is calculated at different gate voltages of 2 000 V, 3 000 V, and 5 000 V respectively. The emission current from gated CNT increases exponentially with increasing of the gate voltage. The emission current from gated CNT versus 2 000 V, 3 000 V, and 5 000 V is 89.62 μA, 132.72 μA, and 267.39 μA respectively as the gate voltage is 200 V.

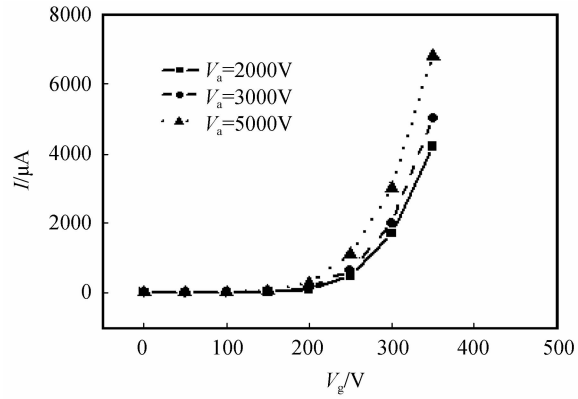

Fig. 14 The plots of field emission current as a function of gate voltage V_g at different anode voltates

4 Conclusion

In this study, the potential distribution near the top of CNT, the actual electric field and the field enhancement factor at the top of CNT, and the field emission current from gated CNT are calculated analytically based on the superposition principle of electric field with floating spheres model. The actual electric field and the field enhancement factor at the top of CNT are expressed by $E_a=\lambda\cdot V_a+\eta\cdot V_g-IR_0/r_0$ and $\beta=3+\rho+W$ respectively, and the influences of the contact resistance, the geometrical parameters of device, and the dielectric between the gate and cathode for field emission properties are investigated. The theoretical calculation results could provide useful information for the fabrication and the design of the gated carbon nanotube cold cathode field emission displays panels and other nanoscale triode devices.

References

[1] MILNE W I, TEO K B K, CHHOWALLA M, *et al*. Electron emission from arrays of carbon nanotubes/fibres[J]. *Current Applied Physics*, 2002, **2**(6): 509-513.

[2] PIRIO G, LEGAGNEUX P, PRIBAT D, *et al*. Fabrication and electrical characteristics of carbon nanotube field emission microcathodes with an integrated gate electrode [J]. *Nanotechnology*, 2002, **13**(1):1-4.

[3] MINH P N, TUYEN L T T, ONO T, *et al*. Selective growth of carbon nanotubes on Si microfabricated tips and application for electron field emitters[J]. *Journal of Vacuum Science & Technology B*, 2003, **21**(4):1705-1709.

[4] CHOI J H, CHOI S H, HAN J H, *et al*. Enhanced electron emission from carbon nanotubes through density control using in situ plasma of catalyst metal[J]. *Journal of Applied Physics*, 2003, **94**(1): 487-490.

[5] CHEN Qi-dao and DAI Li-ming. Three-dimensional micropatterns of well-aligned carbon nanotubes produced by photolithography [J]. *Journal of Nanoscience and Nanotechnology*, 2001, **1**(1): 43-47.

[6] LEE Y H, JANG Y T, KIM D H, *et al*. Realization of gated field emitters for electrophotonic applications using carbon nanotube line emitters directly grown into submicrometer holes [J]. *Advanced Materials*, 2001, **13**(7): 479-482.

[7] TEO K B K, CHHOWALLA M, AMARATUNGA G A, *et al*. Field emission from dense, sparse, and patterned arrays of carbon[J]. *Applied Physics Letters*, 2002, **80**(11): 2011-2013.

[8] HSU D S Y. Microgating carbon nanotube field emitters by in-situ growth inside open aperture arrays[J]. *Applied Physics Letters*, 2002, **80**(16): 2988-2992.

[9] HSU D S Y, SHAW J. Integrally gated carbon nanotube-on-post field emitter arrays[J]. *Applied Physics Letters*, 2002, **80**(1): 118-121.

[10] PARK K H, SEO W J, LEE S, *et al*. Triode field emitter with a gated planar carbon-nanoparticle cathode[J]. *Applied Physics Letters*, 2002, **81**(2): 358-360.

[11] WANG Xin-qing, WANG Miao, LI Zhen-hua, *et al*. Modeling and calculation of field emission enhancement factor for carbon nanotubes array[J]. *Ultramicroscopy*, 2005, **102**(3): 181-186.

[12] ZhENG X, CHEN G H, LI Z B, *et al*. Quantum-mechanical investigation of field-emission mechanism of a micrometer-long single-walled carbon nanotube[J]. *Physical Review Letters*, 2004, **92**(10): 106803.

[13] BULDUM A, LU J P. Electron field emission properties of closed carbon nanotubes[J]. *Physical Review Letters*, 2003, **91**: 236801.

[14] LAN Y C, LEE C T, HU Y, *et al*. Simulation study of carbon nanotube field emission display with under-gate and planar-gate structures[J]. *Journal of Vacuum Science & Technology B*, 2004, **22**(3): 1244-1249.

[15] WONG Y M, KANG W P, DAVIDSON J L, *et al*. Array geometry, size and spacing effects on field emission characteristics of aligned carbon nanotubes[J]. *Diamond and Related Materials*, 2005, **14**(11-12): 2078-2083.

[16] NICOLAESCU D, FILIP V, KANEMARU S, *et al*. Modeling of field emission nanotriodes with carbon nanotube emitters[J]. *Journal of Vacuum Science & Technology B*, 2003, **21**(1): 366-374.

[17] LEI Da, ZENG Le-yong, WANG Wei-biao, *et al*. Model calculation for enhancement factor of a gated field emission Nanotube[J]. *Journal of Applied Physics*, 2007, **102**(11): 1-5.

[18] LEI Da, WANG Wei-biao, ZENG Le-yong, *et al*. Calculation of electron emission from a gated single nanowire [J]. *Journal of Vacuum Science & Technology B*, 2009, **27**(5): 2217-2221.

[19] SHE Jun-cong, XU Ning-shen, DENG Shao-zhi, *et al*. Vacuum breakdown of carbon-nanotube field emitters on a silicon tip[J]. *Applied Physics Letters*, 2003, **83**(13): 2671-2673.

[20] MILLER H C. Change in field intensification factor beta of and electrode projection (Whisker) at short gap lengths[J]. *Journal of Applied Physics*, 1967, **38**(11): 4501-4504.